Int. J. Radiation Oncology Biol. Phys., Vol. 82, No. 5, pp. 1715–1722, 2012

0360-3016/$ - see front matter

ELSEVIER

doi:10.1016/j.ijrobp.2011.03.034

PHYSICS CONTRIBUTION

MEGAVOLTAGE CONE BEAM COMPUTED TOMOGRAPHY DOSE AND THE NECESSITY OF REOPTIMIZATION FOR IMAGING DOSE-INTEGRATED INTENSITY-MODULATED RADIOTHERAPY FOR PROSTATE CANCER

YUICHI AKINO, M.S.,* MASAHIKO KOIZUMI, M.D.,† IORI SUMIDA, PH.D.,*† YUTAKA TAKAHASHI, PH.D.,*† TOSHIYUKI OGATA, M.S.,*† SEIICHI OTA, B.S.,‡ FUMIAKI ISOHASHI, M.D.,* KOJI KONISHI, M.D.,* AND YASUO YOSHIOKA, M.D.*

*Department of Radiation Oncology, Osaka University Graduate School of Medicine, Suita, Osaka, Japan; †Division of Medical Physics, Oncology Center, and ‡Division of Radiology, Department of Medical Technology, Osaka University Hospital, Suita, Osaka, Japan

Purpose: Megavoltage cone beam computed tomography (MV-CBCT) dose can be integrated with the patient's prescription. Here, we investigated the effects of imaging dose and the necessity for additional optimization when using intensity-modulated radiotherapy (IMRT) to treat prostate cancer.

Methods and Materials: An arc beam mimicking MV-CBCT was generated using XiO (version 4.50; Elekta, Stockholm, Sweden). The monitor units (MU) for dose calculation were determined by conforming the calculated dose to the dose measured using an ionization chamber. IMRT treatment plans of 22 patients with prostate cancer were retrospectively analyzed. Arc beams of 3, 5, 8, and 15 MU were added to the IMRT plans, and the dose covering 95% of the planning target volume (PTV) was normalized to the prescribed dose with (reoptimization) or without optimization (compensation).

Results: PTV homogeneity and conformality changed negligibly with MV-CBCT integration. For critical organs, an imaging dose-dependent increase was observed for the mean rectal/bladder dose (D_{mean}), and reoptimization effectively suppressed the D_{mean} elevations. The bladder generalized equivalent uniform dose (gEUD) increased with imaging dose, and reoptimization suppressed the gEUD elevation when 5- to 15-MU CBCT were added, although rectal gEUD changed negligibly with any imaging dose. Whereas the dose elevation from the simple addition of the imaging dose uniformly increased rectal and bladder dose, the rectal D_{mean} increase of compensation plans was due mainly to low-dose volumes. In contrast, bladder high-dose volumes were increased by integrating the CBCT dose, and reoptimization reduced them when 5- to 15-MU CBCT were added.

Conclusion: Reoptimization is clearly beneficial for reducing dose to critical organs, elevated by addition of high-MU CBCT, especially for the bladder. For low-MU CBCT aimed at bony structure visualization, compensation is sufficient. © **2012 Elsevier Inc.**

Dose compensation, Megavolt cone beam computed tomography, Prostate IMRT, Reoptimization.

INTRODUCTION

Megavoltage cone beam computed tomography (MV-CBCT) using a MV treatment beam and an electronic portal imaging device enables precise quantitative evaluation of patient setup error (1–3). The technology allows verification of organ alignment and estimation of the actual dose delivered to patients (4–6). Advantages of MV-CBCT include its stable geometry and low incidence of metal artifacts compared to kilovoltage CBCT (kV-CBCT). Disadvantages include elevated dose (7) and low image contrast compared to kV-CBCT (8), although improvements to the latter have been made (9, 10).

Intensity-modulated radiotherapy (IMRT) allows a reduction in the dose to organs at risk (OARs) by modulating the beam intensity in each beam field, using a multileaf collimator (11, 12). Pelvic organs exhibit both systematic and random motions, deformations, and size variations during treatment and over the entire course of therapy (13–16). Achieving the desired dose distribution requires still more accurate patient setup, as any uncertainty will be

Reprint requests to: Masahiko Koizumi, M.D., Ph.D., Division of Medical Physics, Oncology Center, Osaka University Hospital, 2-2(D10), Yamadaoka, Suita, Osaka, 565-0871, Japan. Tel: (+81) 6 6879 3482; Fax: (+81) 6 6879 3489; E-mail: koizumi@radonc.med.osaka-u.ac.jp

Conflict of interest: none.

Acknowledgment—This work was supervised by the late Takehiro Inoue, Professor, Department of Radiation Oncology, Osaka University Graduate School of Medicine. We gratefully thank him for his wise counsel regarding the design, analysis, and reporting of this study.

Received May 11, 2010, and in revised form Feb 10, 2011. Accepted for publication March 22, 2011.

accompanied by deformation of dose distribution, resulting in the failure of dose delivery to targets and elevated dose to OARs (17). For setup verification in our institution, we routinely used a monitor unit (MU) value of 3 for CBCT, which is the minimum value for image acquisition protocols. We verified that the image quality of 3-MU CBCT was adequate for recognizing skeletal structures. For soft tissue visualization, however, we consider that 8 or more MU are required, based on clinical experience. Similarly, Morin et al. (1, 18) have suggested that the image contrast of 9-MU CBCT is sufficient for soft tissue visualization. Typically, an IMRT series consists of many fractions, and the contribution of the MV-CBCT dose may be unacceptable if image acquisition with high MU is applied to every treatment fraction. The characteristics of the CBCT beam are quite similar to those of the treatment beam, meaning that MV-CBCT dose distribution can be estimated using a radiotherapy treatment planning system (RTPS) (2). Morin et al. (18) introduced a methodology for integrating MV-CBCT dose with the prescribed dose, which used 5 MU for the head and neck region and 9 MU for the pelvic region. Those imaging doses were integrated into prescribed doses for radiotherapy by scaling down the dose weights from the total prescribed dose of the treatment beams. Miften et al. (19) showed that IMRT optimization performed after addition of the MV-CBCT beam reduced OAR dose by taking into consideration the contribution of the MV-CBCT beam. That study's MV-CBCT protocols used 15 MU for the pelvic region. The MU values for MV-CBCT were fixed in those studies, and no study has investigated the effects of MU alteration on dose distribution, although imaging dose is known to affect both patient dose and MV-CBCT image quality (2, 20).

Here, we investigated the effects of MV-CBCT imaging dose alteration and the necessity for reoptimizing MV-CBCT dose-integrated IMRT related to dose distribution in treating prostate cancer.

METHODS AND MATERIALS

Linear accelerator and MV-CBCT system

Our institution's Oncor Impression Plus linear accelerator (LINAC) with Optifocus multileaf collimator (both from Siemens Medical Solutions, Concord, CA) is capable of generating dual-energy X-ray beams (6 and 10 MV). An MVision MV-CBCT system (Siemens Medical Solutions) was installed. During MV-CBCT acquisition, the gantry of the LINAC rotates from 270° to 110°, generating a 6-MV photon beam. The field width of the MV-CBCT system is 27.4 cm. The maximum range in the superior-inferior direction is 27.4 cm, and the range can be adjusted using Y-jaws.

Dose calculation and verification of MV-CBCT accuracy

Dose distribution for MV-CBCT and treatment planning was done using an XiO version 4.50 (Elekta, Stockholm, Sweden) treatment planning system. The MV-CBCT system with doses of 3, 5, 8, and 15 MU (set MU) was calculated by regarding it as an arc beam with a gantry rotation from 270° to 110°. The calculation step of the arc beam was 10°. Field length along the Y-axis (superior-inferior direction) was 9 cm for the phantom study. The accuracy of dose calculation was verified by measurement using an I'm*RT* Phantom (IBA Dosimetry GmbH, Schwarzenbruck, Germany); a 0.6-cc Farmer-type ionization chamber, model TN30013 (PTW, Freiburg, Germany); and Gafchromic EBT2 film (International Specialty Products, Wayne, NJ).

For calculation, the I'm*RT* Phantom's electron density was considered equivalent to that of water, and the measured values were corrected using a solid phantom-to-water dose conversion factor (21). Point dose in the phantom was measured at nine points, namely the center of the phantom and points shifted vertically and horizontally by ±3 cm (Fig. 1A). To investigate the dose distribution of MV-CBCT alone, Gafchromic film in the I'm*RT* Phantom was irradiated ten times. To simulate clinical use, films were irradiated with MV-CBCT, as well as the series of IMRT beams from one patient. The summed dose distribution was analyzed. For analysis of radiochromic films, three-channel data (red-green-blue) were acquired at 150 dpi, using a flatbed scanner (model ES-10000G; Epson Seiko Corp., Nagano, Japan). We used software developed inhouse to extract red channel data from scanned images and converted them to dose distribution data, using dose calibration curve prepared for EBT2 films. We confirmed that the difference in responses of EBT2 film to 6 MV and 10 MV X-radiation was negligibly small (data not shown), and therefore, we used the calibration curve prepared using 10 MV X-rays for the analysis of films. The planar dose maps extracted from films and exported from XiO were imported into MapCHECK version 5.01.02 software (Sun Nuclear, Melbourne, FL), and the differences between dose distribution measured by films and that calculated by XiO were evaluated using the γ index (22).

Patients and IMRT planning

We retrospectively analyzed the treatment plans of 22 patients with intermediate- or high-risk prostate cancer, who were treated with IMRT between March and November 2009. A radiation oncologist delineated the prostate and seminal vesicles of all patients. The clinical target volume (CTV) was generated for the prostate and part of the seminal vesicles, and the overlapping region of the CTV with margins for all directions and rectum was then subtracted and defined as the planning target volume (PTV).

OARs were contoured by medical physicists and reviewed by a radiation oncologist. Bladder and rectal volumes were defined as solid structures within the external organ contour. The rectum was delineated from the rectosigmoid junction to the level of the ischial tuberosity or the anus. The prescribed dose was 74 Gy/37 fractions. PTV and OAR volume information for the patients is listed in Table 1. A five-field coplanar treatment plan with beam angles of 45°, 105°, 180°, 255°, and 315° was generated using a 10-MV photon beam for each patient. After optimization, the final dose was calculated using a fast Fourier transform convolution algorithm with a grid size of 2.0 mm.

Imaging dose integration and reoptimization of the IMRT plan

For all patients' IMRT plans, the dose covering 95% of PTV (D95) was normalized to the prescribed dose (74 Gy). To create simple addition plans, an arc beam mimicking 6-MV CBCT was added to the clinically approved treatment plan of each patient. The craniocaudal CBCT imaging range was 10 cm. The D95 value from total beams clearly exceeded the prescribed dose.

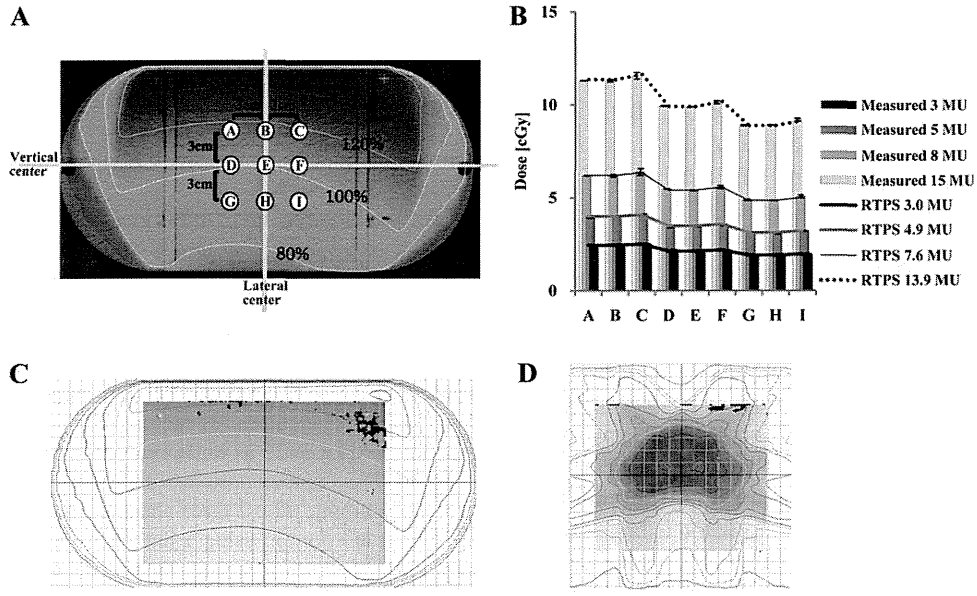

Fig. 1. (A) Dose distribution of MV-CBCT and location for measurement of point-dose using an ion chamber is shown. The axial plane of the I'm*RT* Phantom, displaying measurement points, is shown. Isodose lines show relative dose to the isocenter as calculated by using a XiO system. (B) MV-CBCT dose comparisons between measurements and calculations are shown. The horizontal axis corresponds to the location in panel A. Columns and bars represent means ± standard deviations (SDs) for measurements. The lines indicate the calculated values. The γ analysis using EBT2 film for (C) 15-MU CBCT alone and (D) IMRT beams with 3-MU CBCT of a representative patient is shown. The criterion of γ analysis is 3%/3 mm, and the region exceeding the criterion is red. The dose distributions of films and calculations are shown as gray-scale and lines, respectively.

Two further treatment plan types were created, one involving an additional round of IMRT-beam optimization (reoptimization plans) and a second without this additional optimization (compensation plans). To create compensation plans, the total dose was normalized to D95 by simple rescaling of IMRT beam weights, keeping imaging doses constant. For reoptimization plans, another optimization was performed after adding MV-CBCT. The dose constraints for reoptimization were not altered from the clinically approved treatment plans to eliminate any differences with regard to planner's individual techniques. After optimization, PTV D95 was normalized to the prescribed dose.

To assess the effects of daily portal imaging without incorporating imaging dose into the prescribed dose, two orthogonal beams mimicking portal imaging beams were created in the RTPS. The energy, field size, and imaging MU values for the portal imaging beams were 6 MV, 15 × 15 cm^2, and 1 MU, respectively, for both anterior-posterior and lateral beams. Total numbers of fractions were equal for portal imaging and IMRT. Dose calculation accuracy, linearity, and repeatability for X-ray beams with small MU were verified monthly.

Plan evaluation

To evaluate target coverage quality, PTV homogeneity (*HI*) and conformity (*CI*) indices were calculated using the following formulas:

$$HI = D_{\max}/D_{\min}$$

and

$$CI = V_{Rx}/V_{PTV}$$

where $D_{\max}$, $D_{\min}$, V_{Rx}, and V_{PTV} represent maximum dose, minimum dose, prescription isodose volume, and the PTV volume, respectively. *HI* represents the increase or decrease of hot and cold regions. The values are close to unity for homogenous plans and are large for inhomogeneous plans. *CI* stands for plan conformality. In this study, PTV D95 was normalized to the prescribed dose and was never changed by compensation and reoptimization. *CI* therefore stands for the ineffective dose delivered around PTV. *CI* values are close to unity for conformal plans and become larger for nonconformal plans.

For OARs, rectal and bladder mean doses (D_{mean}) were calculated as follows:

$$D_{mean} = \sum_i \frac{D_i V_i}{V}$$

where V_i is the volume receiving a certain dose (D_i), and V stands for total volume. To evaluate the variations of radiobiological effects from the imaging dose, the generalized equivalent uniform dose (gEUD) proposed by Niemierko (23) for each OAR was also calculated, as follows:

$$gEUD = \left(\sum_i \frac{V_i}{V} D_i^{1/n} \right)^n$$

where n is a parameter that describes the volumetric dependence of the dose-response relationship for each organ. When n = 1, the

Table 1. Patient information and calculated dose of MV-CBCT for each patients

	Volume (cc)			MV-CBCT dose (cGy)			
Dose	PTV	Rectum	Bladder	3 MU	5 MU	8 MU	15 MU
Median	71.9	42.4	132.9	80.8	131.9	204.6	374.1
Minimum	52.9	28.8	23.2	77.1	125.9	195.3	357.1
Maximum	136.9	61.3	363.0	85.4	139.6	216.5	395.9

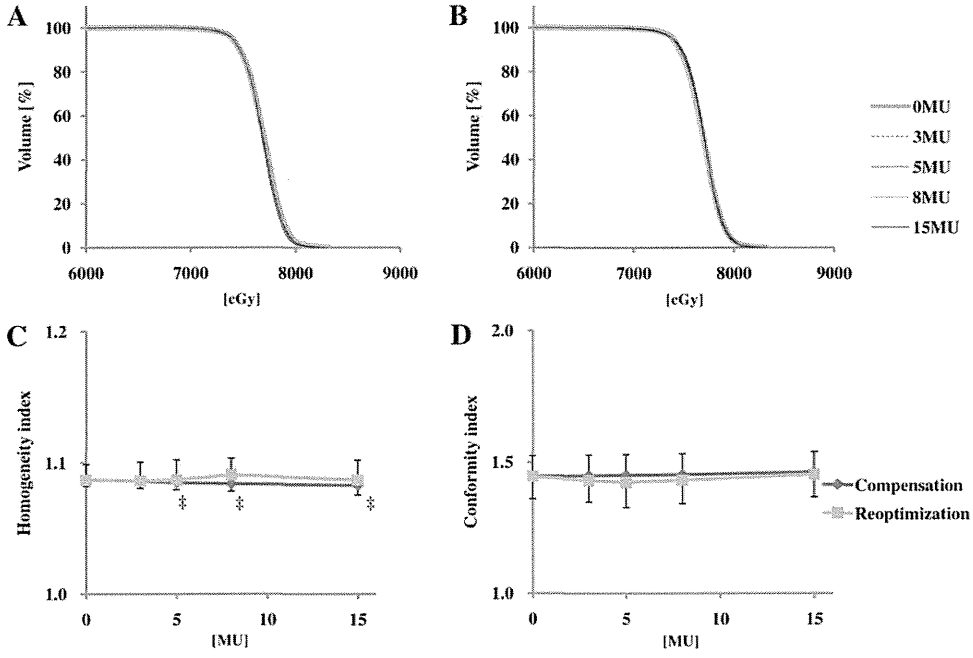

Fig. 2. Evaluation of the effects of MV-CBCT integration and reoptimization of PTV dose coverage. Representative DVHs for (A) compensation plans and (B) reoptimization plans are shown. PTV homogeneity (C) and conformity (D) indices are shown: imaging-MU is plotted along the x-axis and points and bars represent median and interquartile ranges, respectively. †, $p < 0.05$; ‡, $p < 0.01$. (Paired *t*-tests show a comparison between compensation and reoptimization plans with the same MU).

gEUD value is equal to D_{mean}, and a lower n value indicates stronger high-dose sensitivity. The gEUD represents the homogeneous dose distribution that results in the same probability of complications as that of an inhomogeneous dose distribution. The values of n were 0.12 and 0.5 for rectum and bladder, respectively, as Burman et al. previously reported (24). The rectal and bladder volumes receiving a certain dose (Vx) were also analyzed. For calculating D_{mean}, gEUD, and Vx, the dose-volume data were derived from dose-volume histogram (DVH) data exported from RTPS.

Statistical analyses

Statistical significance was assessed using the paired *t*-test, and statistical significance was set at a p value of <0.05. The Bonferroni correction was used for multiple comparison.

RESULTS

MV-CBCT dose calculation accuracy

The monitor chamber mounted on the LINAC indicated values (actual MU) of 2.7 ± 0.0, 4.5 ± 0.0, 7.2 ± 0.0, and 13.3 ± 0.1 MU for MV-CBCT beams with set MU of 3, 5, 8, and 15 MU, respectively. In a preliminary study using actual MU for calculations, unacceptable calculation errors (>10%) were observed, particularly for low-MU CBCT, although the treatment arc beam was calculated accurately (data not shown). In our study, the imaging MU values for calculations were determined by conforming the calculated dose to the dose measured using the ionization chamber. The doses from MV-CBCT for 3, 5, 8, and 15 MU (set MU) measured at the center of I′m*RT* Phantom corresponded to 3.0, 4.9, 7.6, and 13.9 MU, respectively, determined by using the XiO system. MV-CBCT doses measured by the ionization chamber and calculated by the RTPS are compared in Fig. 1B. For all eight points around the center of the I′m*RT* Phantom (Fig. 1B, point E), the error between the measured and calculated doses was less than 1.3% for all imaging MU, and the maximum absolute error was 0.08 cGy.

We also assessed MV-CBCT dose distribution calculation accuracy along the axial plane in the I′m*RT* Phantom (Fig. 1C and D). The criterion of γ analysis is 3%/3 mm, and the region exceeding the criterion was colored red. The CBCT dose distribution agreed well with the calculation (Fig. 1C). To assess the calculation accuracy for clinical use, two-dimensional dose distributions of MV-CBCT combined with IMRT beams were measured using film and compared with the calculation. The representative result using 3-MU CBCT is shown in Figure 1D. Almost all regions passed the criterion for any MU. The pass rate was greater than 98% for CBCT with or without IMRT.

Effect of reoptimization on PTV homogeneity and conformality

Figure 2A and B shows the PTV DVH for compensation and reoptimization plans, respectively. One patient with PTV and OAR volumes close to the median values was chosen. For both techniques, the curves of plans with 3- to 15-MU CBCT were highly similar to those of the nonimaging plan (0 MU), indicating little change in PTV coverage. Figure 2C and D shows PTV *HI* and *CI* indices, respectively. For *HI*, no significant differences were noted for both techniques compared with nonimaging values. Compensation with 5 to 15 MU showed a statistically significant decrease

of *HI* compared to reoptimization, although the amplitude was small. The change in *CI* was not statistically significant for any imaging dose.

Effects of reoptimization on OAR dose

Figure 3A illustrates changes in the rectal D_{mean} value from nonimaging values. While both compensation and reoptimization plans showed an imaging dose-dependent increase in rectal D_{mean}, reoptimization significantly suppressed dose elevation by half compared with compensation ($p < 0.001$ for all MU). Whereas the D_{mean} value of compensation plans became larger than observed with portal imaging when 8- to 15-MU CBCT was added, the D_{mean} value of reoptimization plans did not exceed that of portal imaging. Figure 3B shows the changes in gEUD from nonimaging plans. For the simple addition of portal imaging and 3-MU CBCT, the amplitude of gEUD elevation was similar to that of D_{mean}. In contrast, gEUD determined by both techniques changed modestly with every imaging dose. Because gEUD reflects the effect of inhomogeneous dose distribution, the cause of the disagreement seen in these results may be found in the dose-volume analysis (Fig. 3C). The rectal *Vx* value was uniformly elevated by addition of portal imaging and 3-MU CBCT. In contrast, compensation plans showed a remarkable increase of low-dose volume (V30–V50), while the changes in high-dose volume (V60–V70) were modest. The *Vx* elevations, especially those of low-dose volumes, were suppressed by reoptimization. No significant difference was noted between V60 for compensation and reoptimization plans when 3-MU CBCT was added, and there was no significant difference in V70 for all MU.

Figure 4 shows results for bladder doses subjected to the same analyses as those conducted above. The bladder D_{mean} value was also increased with increasing imaging dose (Fig. 4A). Unlike the results for the rectum, however, gEUD increased significantly for compensation and reoptimization plans compared with nonimaging values (Fig. 4B), and reoptimization significantly suppressed the gEUD elevation when 5 to 15 MU were added ($p = 0.008$ and 0.001 and $p < 0.001$ for 5 and 8 and 15 MU, respectively). As the analysis of *Vx* (Fig. 4C) shows, V70 was increased with increasing CBCT dose, and reoptimization significantly suppressed V70 elevation when 5 to 15 MU

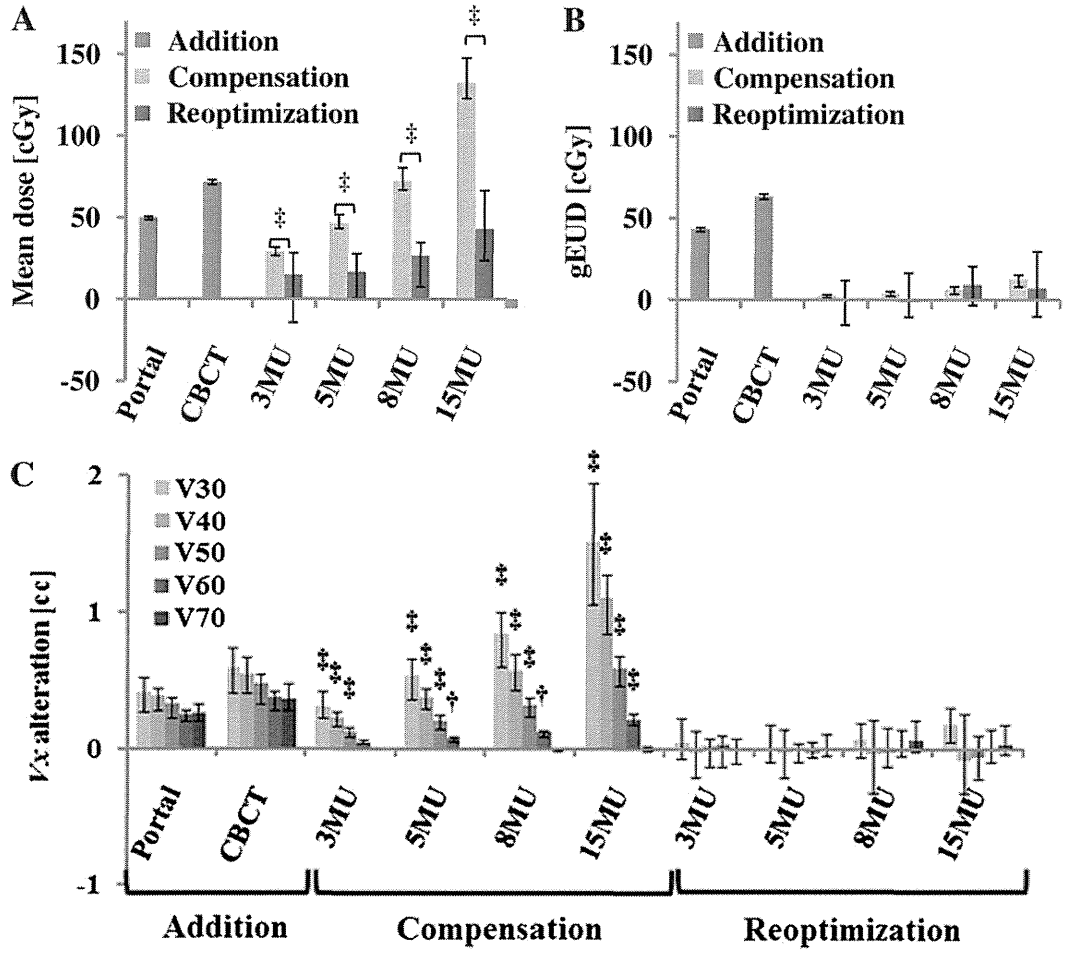

Fig. 3. The effects of MV-CBCT integration on rectal dose. The D_{mean} (A), gEUD (B), and *Vx* (C) values are shown. Each value represents the change from those of nonimaging plans. Columns and bars represent median and interquartile range, respectively. †, $p < 0.05$; ‡, $p < 0.01$. (Paired *t*-test comparisons between compensation and reoptimization plans with the same MU are shown).

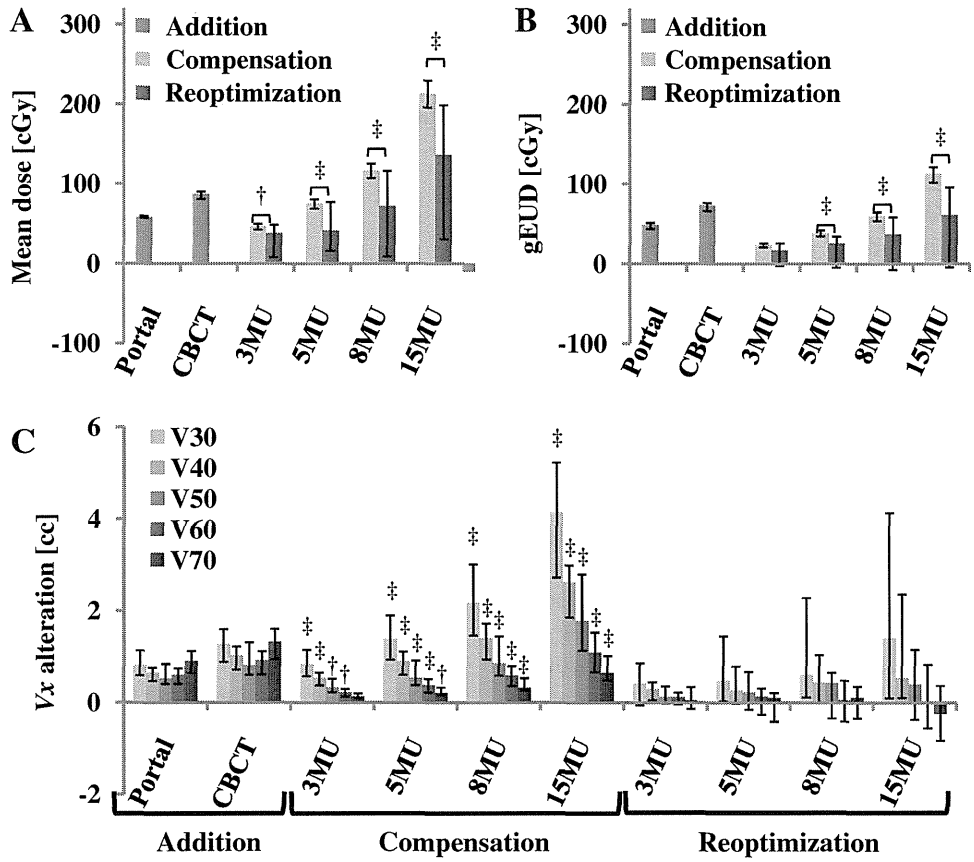

Fig. 4. The effects of MV-CBCT integration on bladder dose are shown. The D_{mean} (A), gEUD (B), and *Vx* (C) values are shown. Each value represents the change from those of nonimaging plans. Columns and bars represent median and interquartile range, respectively. †, $p < 0.05$; ‡, $p < 0.01$. (Paired *t*-test comparisons between compensation and reoptimization plans with the same MU are shown).

were added ($p = 0.044$ and 0.009 and $p < 0.001$ for 5 MU and 15 MU, respectively).

DISCUSSION

The accurate calculation of MV-CBCT dose distribution is essential to the integration of imaging dose with prescribed dose. Here, we were able to accurately calculate MV-CBCT dose distribution by using our method, even for quite low MU (Fig. 1B–D). We confirmed the fact that this method also allowed the accurate calculation of dose in differently shaped phantoms and that the stability of the MV-CBCT beam output was ensured by weekly measurement, routinely performed for IMRT quality assurance. We conclude that our method is feasible for any imaging dose, if the stability of beam output is confirmed by scheduled measurements. Similarly, the report of the American Association of Physicists in Medicine Task Group 142 recommended annual or more frequent assessment of imaging dose (25).

Regarding target coverage, compensation plans showed slightly decreased *HI* (Fig. 2C), indicating a decrease in hot or cold regions in the target volume. This is attributed to the uniform dose distribution of the MV-CBCT dose. However, the alteration was quite small and might be considered clinically negligible. Because the results of *HI* and *CI* demonstrated that MV-CBCT dose integration with both techniques did not worsen the quality of target coverage, the necessity of reoptimization can be simply evaluated by considering the effects of imaging dose on critical organs.

For the rectal D_{mean} value, reoptimization seemed to have a significant advantage for suppressing rectal dose elevation upon addition of imaging dose, particularly for high-MU CBCT (Fig. 3A). However, gEUD values for both techniques showed negligible changes from nonimaging values (Fig. 3B). The results of dose-volume analysis (Fig. 3C) explain the cause of the disagreement: compensation plans mainly increased low-dose volume (30–50 Gy), while their alteration of high-dose volume was modest. In contrast, simple addition of both portal imaging and 3-MU CBCT uniformly increased rectal *Vx*. In general, rectal complications result from high doses (26). Although many studies have demonstrated the association of late rectal toxicity with high dose (≥60 Gy), rectal bleeding correlates with the volume exposed to intermediate doses (40–60 Gy) (26, 27). Jackson et al. (27) stated that the intermediate dose might be associated with the recovery of tissue exposed to high dose. While compensation might be sufficient for reducing rectal injury, reoptimization could still be beneficial for reducing the volume receiving intermediate dose.

Although MV-CBCT dose increased both rectal and bladder D_{mean} values, the amplitude of the bladder dose elevation was larger than that of the rectal dose (Figs. 3A and 4A). The dose distribution of MV-CBCT is arch-shaped, indicating that the anterior region receives a relatively higher dose than the isocenter (Fig. 1A). Interestingly, the bladder but not rectal gEUD value increased with imaging dose. As Figure 4C shows, a significant increase in bladder V60 to V70 was observed in compensation plans. This increase can also be explained by the arch-shaped dose distribution of MV-CBCT. When PTV D95 is normalized to the prescribed dose by scaling down IMRT beams, insufficient compensation will result in the increased bladder dose, even for high *Vx*. Reoptimization significantly reduced bladder gEUD by modifying beam intensity and reduced high-dose volume (V60–V70) when 5 to 15 MU were added. Although little information about dose-volume relationship related to genitourinary toxicity was provided, Zelefsky et al. (28) reported a 20% incidence in late Grade ≥2 toxicity after 81-Gy prostate IMRT compared to a 12% incidence for non-IMRT patients treated with lower doses. While conformal RT techniques enable dose escalation, the bladder receives a localized but higher dose than with conventional RT. In patients in whom frequent MV-CBCT acquisition with high MU elevates the dose to this organ, reoptimization will be beneficial in reducing the risk of complications.

CONCLUSIONS

Many institutions may use MV-CBCT less frequently (*i.e.*, once weekly) or with low MU (*i.e.*, 3–5 MU) because of increased dose to normal tissue. For institutions using portal imaging for daily setup, portal imaging can be replaced by 3-MU CBCT because its dose is low and close to that of portal imaging. However, dose compensation is still valuable for reducing OAR dose. In that case, the low-MU CBCT calculation method described here would facilitate dose compensation. As our present study shows, compensation is sufficient for reducing the OAR dose increased by low-MU CBCT, and reoptimization is unnecessary. In contrast, for high-MU CBCT, reoptimization is obviously beneficial for reducing OAR dose, especially for the bladder. Appropriate application of these measures should allow accurate treatment with smaller PTV margins that result in fewer complications.

REFERENCES

1. Morin O, Gillis A, Chen J, *et al.* Megavoltage cone-beam CT: System description and clinical applications. *Med Dosim* 2006; 31:51–61.
2. Gayou O, Parda DS, Johnson M, *et al.* Patient dose and image quality from mega-voltage cone-beam computed tomography imaging. *Med Phys* 2007;34:499–506.
3. Gayou O, Miften M. Commissioning and clinical implementation of a mega-voltage cone beam CT system for treatment localization. *Med Phys* 2007;34:3183–3192.
4. Bylund KC, Bayouth JE, Smith MC, *et al.* Analysis of interfraction prostate motion using megavoltage cone beam computed tomography. *Int J Radiat Oncol Biol Phys* 2008;72: 949–956.
5. Aubry JF, Cheung J, Morin O, *et al.* Correction of megavoltage cone-beam CT images of the pelvic region based on phantom measurements for dose calculation purposes. *J Appl Clin Med Phys* 2009;10:33–42.
6. Petit SF, van Elmpt WJ, Lambin P, *et al.* Dose recalculation in megavoltage cone-beam CT for treatment evaluation: removal of cupping and truncation artifacts in scans of the thorax and abdomen. *Radiother Oncol* 2010;94:359–366.
7. Peng LC, Yang CC, Sim S, *et al.* Dose comparison of megavoltage cone-beam and orthogonal-pair portal images. *J Appl Clin Med Phys* 2007;8:10–20.
8. Stützel J, Oelfke U, Nill S. A quantitative image quality comparison of four different image guided radiotherapy devices. *Radiother Oncol* 2008;86:20–24.
9. Faddegon BA, Wu V, Pouliot J, *et al.* Low dose megavoltage cone beam computed tomography with an unflattened 4 MV beam from a carbon target. *Med Phys* 2008;35:5777–5786.
10. Flynn RT, Hartmann J, Bani-Hashemi A, *et al.* Dosimetric characterization and application of an imaging beam line with a carbon electron target for megavoltage cone beam computed tomography. *Med Phys* 2009;36:2181–2192.
11. Ezzell GA, Galvin JM, Low D, *et al.* Guidance document on delivery, treatment planning, and clinical implementation of IMRT: Report of the IMRT subcommittee of the AAPM radiation therapy committee. *Med Phys* 2003;30:2089–2115.
12. Galvin JM, Ezzell G, Eisbrauch A, *et al.* Implementating IMRT in clinical practice: A joint document of the American Society for Therapeutic Radiology and Oncology and the American Association of Physicists in Medicine. *Int J Radiat Oncol Biol Phys* 2004;58:1616–1634.
13. Antolak JA, Rosen II, Childress CH, *et al.* Prostate target volume variations during a course of radiotherapy. *Int J Radiat Oncol Biol Phys* 1998;42:661–672.
14. Zellars RC, Roberson PL, Strawderman M, *et al.* Prostate position late in the course of external beam therapy: Patterns and predictors. *Int J Radiat Oncol Biol Phys* 2000;47:655–660.
15. de Crevoisier R, Melancon AD, Kuban DA, *et al.* Changes in the pelvic anatomy after an IMRT treatment fraction of prostate cancer. *Int J Radiat Oncol Biol Phys* 2007;68:1529–1536.
16. Adamson J, Wu Q. Inferences about prostate intrafraction motion from pre- and posttreatment volumetric imaging. *Int J Radiat Oncol Biol Phys* 2009;75:260–267.
17. van Haaren PM, Bel A, Hofman P, *et al.* Influence of daily setup measurements and corrections on the estimated delivered dose during IMRT treatment of prostate cancer patients. *Radiother Oncol* 2009;90:291–298.
18. Morin O, Gillis A, Descovich M, *et al.* Patient dose considerations for routine megavoltage cone-beam CT imaging. *Med Phys* 2007;34:1819–1827.
19. Miften M, Gayou O, Reitz B, *et al.* IMRT planning and delivery incorporating daily dose from mega-voltage cone-beam computed tomography imaging. *Med Phys* 2007;34:3760–3767.
20. Morin O, Aubry JF, Aubin M, *et al.* Physical performance and image optimization of megavoltage cone-beam CT. *Med Phys* 2009;36:1421–1432.
21. Seuntjens J, Olivares M, Evans M, *et al.* Absorbed dose to water reference dosimetry using solid phantoms in the context of absorbed-dose protocols. *Med Phys* 2005;32:2945–2953.

22. Low DA, Harms WB, Mutic S, *et al.* A technique for the quantitative evaluation of dose distributions. *Med Phys* 1998;25: 656–661.
23. Niemierko A. A generalized concept of equivalent uniform dose (EUD). *Med Phys* 1999;26:1100 (Abstract).
24. Burman C, Kutcher GJ, Emami B, *et al.* Fitting of normal tissue tolerance data to an analytic function. *Int J Radiat Oncol Biol Phys* 1991;21:123–135.
25. Klein EE, Hanley J, Bayouth J, *et al.* Task Group 142 report: Quality assurance of medical accelerators. *Med Phys* 2009; 36:4197–4212.
26. Michalski JM, Hiram Gay, Jackson A, *et al.* Radiation dose-volume effects in radiation-induced rectal injury. *Int J Radiat Oncol Biol Phys* 2010;76:S123–S129.
27. Jackson A, Skwarchuk MW, Zelefsky MJ, *et al.* Late rectal bleeding after conformal radiotherapy of prostate cancer. II. Volume effects and dose-volume histograms. *Int J Radiat Oncol Biol Phys* 2001;49:685–698.
28. Zelefsky MJ, Levin EJ, Hunt M, *et al.* Incidence of late rectal and urinary toxicities after three-dimensional conformal radiotherapy and intensity-modulated radiotherapy for localized prostate cancer. *Int J Radiat Oncol Biol Phys* 2008;70:1124–1129.

Journal of Radiation Research, 2012, 53, 722–726
doi: 10.1093/jrr/rrs027 Advance Access Publication 28 June 2012

Dose reduction trial from 60 Gy in 10 fractions to 54 Gy in 9 fractions schedule in high-dose-rate interstitial brachytherapy for early oral tongue cancer

Hironori AKIYAMA[1], Ken YOSHIDA[2], Kimishige SHIMIZUTANI[1], Hideya YAMAZAKI[3,*], Masahiko KOIZUMI[4], Yasuo YOSHIOKA[4], Naoya KAKIMOTO[5], Shumei MURAKAMI[5], Souhei FURUKAWA[5] and Kazuhiko OGAWA[4]

[1]Department of Oral Radiology, Osaka Dental University, 1-5-17, Otemae Chuo-ku, Osaka 540-0008, Japan
[2]Department of Radiation Oncology, National Hospital Organization, Osaka National Hospital, 2-1-14, Hoenzaka, Chuo-ku, Osaka, 540-0006, Japan
[3]Department of Radiology, Graduate School of Medical Science, Kyoto Prefectural University of Medicine, 465 Kajiicho Kawaramachi Hirokoji, Kamigyo-ku, Kyoto 602-8566, Japan
[4]Department of Radiation Oncology, Osaka University Graduate School of Medicine, 2-2, Yamadaoka Suita, Osaka 565-0871, Japan
[5]Department of Oral and Maxillofacial Radiology, Osaka University Graduate School of Dentistry, 2-2, Yamadaoka, Suita, Osaka 565-0871, Japan
*Corresponding author. Department of Radiology, Graduate School of Medical Science, Kyoto Prefectural University of Medicine, 465 Kajiicho Kawaramachi Hirokoji, Kamigyo-ku, Kyoto 602-8566, Japan.
Tel: 81-75-251-5618; Fax: 81-75-251-5840; Email: hideya10@hotmail.com

(Received 28 February 2012; revised 1 May 2012; accepted 7 May 2012)

To compare the effects of 60 Gy/10 fractions (twice a day) with those of 54 Gy/9 fractions in high-dose-rate interstitial brachytherapy (HDR-ISBT) for early tongue cancer, we performed a matched-pair analysis of patients with early tongue cancer (T1-2N0M0), who were treated with 60 or 54 Gy of radiation between 1996 and 2004. Seventeen patients treated with 54 Gy and 34 matched-pair patients treated with 60 Gy were extracted and analyzed. Local recurrence occurred in two patients in the 54-Gy arm and five patients in the 60-Gy arm. The 2-year local control rates were 88% for both the 54-Gy arm and 60-Gy arm (not significant). The 2-year overall survival rates were 88% in the 60-Gy arm and 82% in the 54-Gy arm. Two-year actuarial complication-free rates were 91% in the 60-Gy arm and 83% in the 54-Gy arm (not significant), respectively. There was no significant association between the total dose and local control rate and late complications. The outcome of 54 Gy/ 9 fractions was similar to that of 60 Gy/ 10 fractions in patients with early tongue cancer.

Keywords: tongue cancer; brachytherapy; interstitial radiotherapy; high dose rate

INTRODUCTION

Because radiation therapy is considered to be a minimally invasive treatment procedure, it has the advantage of preserving the shape and functions of the tongue, which vitally affect not only speech but also coordination of chewing and swallowing [1]. Oral tongue carcinoma is highly curable with radiotherapy; therefore, patients are usually treated with low-dose-rate (LDR) interstitial brachytherapy (LDR-ISBT) using ^{137}Cs needles or ^{192}Ir hair pins and a single pin at our hospital [2]. However, because radiation exposure of medical staff cannot be avoided during LDR-ISBT, we introduced a high-dose-rate (HDR) brachytherapy unit comprising a 370-GBq microiridium source that allowed us to use HDR remote afterloading interstitial radiotherapy [3]. On the basis of the results of a Phase I/II study of HDR interstitial radiotherapy [3], 60 Gy in 10 fractions administered over 1 week was selected as the standard schedule for definitive HDR interstitial radiotherapy because early mucosal reactions treated with a total dose of 60 Gy/10 fractions of HDR-ISBT were almost the same as those treated with a total dose of 70 Gy of

LDR-ISBT [4]. Thereafter, we performed a Phase III study, which showed an equivalent outcome for HDR-ISBT and LDR-ISBT. The 5-year local control rates in the LDR and HDR groups were 84% and 87%, respectively, and the 7-year local control rates were 77% and 87%, respectively. There were no differences in the treatment outcomes between the two groups. We concluded that HDR fractionated interstitial brachytherapy can be an alternative to traditional LDR brachytherapy for early tongue cancer.

A few studies have reported the use of HDR-ISBT for the radical treatment of head and neck cancer [5–9]. From a biological standpoint, HDR has the disadvantage of a low therapeutic ratio [10]. However, from the perspective of radiation physics, HDR has the advantage of homogeneous dose distribution. Careful consideration of the advantages and disadvantages of HDR brachytherapy is necessary because some authors have reported lower control rates and higher adverse reaction rates with this form of treatment [5]. Mazeron *et al.* stated that the results of HDR brachytherapy remain to be validated in prospective studies. If it is the only technique available but not included in a prospective study, treatment should be delivered in fractions of <3–4 Gy according to the Groupe Européen de Curiethérapie–European Society for Therapeutic Radiology and Oncology recommendations [1]. Some of the American Brachytherapy Society panel members had concerns about the potential morbidity with fraction sizes as large as 6 Gy delivered to the oral cavity [11], and several reports have shown good outcomes using lower total doses with smaller single fraction doses [5–9]. Our schedule of 60 Gy/10 fractions appeared to be one of the most intensive treatments described in the literature. According to the linear quadratic (LQ) model, an HDR-ISBT dose equivalent to 70 Gy of LDR-ISBT was calculated as 48 Gy in late reaction ($\alpha/\beta = 3.8$) and 54 Gy in acute reaction ($\alpha/\beta = 10$) [12]. A dose of 60 Gy of HDR-ISBT in our schedule is higher than the doses calculated on the basis of the LQ model for 70 Gy of LDR-ISBT. Therefore, we initiated a prospective randomized trial wherein the dose was reduced from 60 Gy to 54 Gy to adjust for 70 Gy of LDR-ISBT ($\alpha/\beta = 10$). However, the number of patients treated in our institution has decreased since 2002, which resulted in difficulty in recruiting enough patients for this phase III study. Because 17 patients have been treated in the 54-Gy arm so far, we performed a case–control matched-pair analysis for the comparison of outcomes between the 54-Gy and 60-Gy schedules.

PATIENTS AND METHODS

Between 1996 and 2005, 51 patients with previously untreated early mobile tongue cancer (T1-2N0) were treated with HDR-ISBT at Osaka University Hospital. Patients treated with combined chemotherapy or external radiotherapy was excluded from the study. The criteria for patient selection for the study were: (i) presence of a T1T2N0 tumor, which could be treated with single-plane implantation; (ii) performance status (World Health Organization) between 0 and 3; and (iii) absence of any severe concurrent disease. All tumors were histologically identified as squamous cell carcinoma. Because we had treated 17 patients with the 54-Gy schedule, we extracted 34 patients treated with the 60-Gy schedule (from 54 patients); these patients were matched by T1/T2 ratio and type of tumor. Table 1 illustrates the characteristics of the patients in the 54-Gy and 60-Gy arms. There were 7 T1 and 10 T2 tumors in the 54-Gy arm and 16 T1 and 18 T2 tumors in the 60-Gy arm (International Union Against Cancer TNM Classification of Malignant Tumors; 1987). The median age was 57 years, with an age range of 28–81 years [54-Gy arm: 56 ± 12 years, 60-Gy arm: 54 ± 13 years, not significant (NS)]. The 54-Gy arm comprised 12 males and 5 females, whereas the 60-Gy arm comprised 26 males and 8 females (NS). All implantations were performed under local anesthesia using 3–16 (median 4) catheters. The treatment method used has been described previously [4]. The patients received a total dose of 54 Gy or 60 Gy in 9 or 10 fractions (6 Gy/fraction), respectively, over 1 week at a 5 mm distance from the radioactive source. Two fractions were administered per day. The time interval between fractions was >6 h. Dose rates at the reference point were 1.0–3.4 Gy/min. Patients were followed up over at least 12 months or until death. The median follow-up duration was 45 months (range: 10–116 months; 52 months for surviving patients). Tumor appearance was classified according to a previous report [4]; there were 7 exophytic, 23 indurative/infiltrative, 14 superficial and 7 ulcerative types. There was no difference in distribution of types between the 54-Gy and 60Gy arms. All patients were enrolled in the study after their informed consent had been obtained prior to radiotherapy in accordance with the guidelines of the intramural ethics committee.

For statistical analysis, Student's *t*-test for normally distributed data and the Mann–Whitney *U*-test for skewed data were used. Percentages were analyzed using the chi-squared test. Local control rates, lymph node control and survival data were estimated according to the Kaplan–Meier method and examined for significance with a logrank test. Results with *P* values <0.05 were considered to be statistically significant.

RESULTS

Seventeen patients treated with 54 Gy and 34 matched-pair control arm patients treated with 60 Gy were analyzed. Seven cases showed local recurrence (two cases in the 54-Gy arm and five cases in the 60-Gy arm). Local control rates for both arms are shown in Fig. 1. The 2- and 3-year local control rates were 88% in both the 54-Gy arm and in the 60-Gy arm, respectively. Local recurrences occurred within 2 years after treatment in six out of the seven cases

Table 1 Patient characteristics

Strata	Variables	60 Gy ($n = 34$)	54 Gy ($n = 17$)	*P*
Gender	Female	8 (24%)	5 (29%)	NS
	Male	26 (76%)	12 (71%)	
Stage	T1	16 (47%)	7 (41%)	NS
	T2	18 (53%)	10 (59%)	
Age		54 ± 13	56 ± 12	NS
Largest diameter	(mm)	23 ± 8	25 ± 8	NS
Thickness	(mm)	7 ± 3	8 ± 6	NS
Technique	Single plane	28 (82%)	13 (76%)	NS
	Double plane	5 (15%)	3 (18%)	
	Volume implant	1 (3%)	1 (6%)	
Type of tumor	Superficial	10 (29%)	4 (24%)	NS
	Exophytic	4 (12%)	3 (18%)	
	Indurative	16 (47%)	7 (41%)	
	Ulcerative	4 (12%)	3 (18%)	
Follow-up periods	(month)	52 (12–116)	44 (13–112)	NS

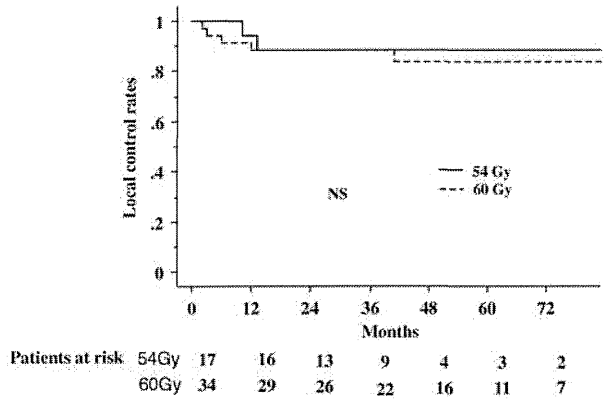

Fig. 1. Local control rates of early tongue carcinoma treated with 60-Gy and 54-Gy interstitial radiotherapy.

Table 2 Treatment results of interstital brachytherapy for early oral tongue cancer using 60 Gy and 54 Gy radiation doses

	60 Gy	54 Gy
Local failure	5	2
Nodal metastasis	13	9
Death	5[a]	4
Late complications		
Soft tissue ulcer	1 (3%)	1 (6%)
Bone exposure	1 (3%)	0 (0%)
Both	2 (6%)	2 (12%)

[a]One death from unknown causes.

with recurrence. In the 60-Gy arm, one patient developed local recurrence 41 months later. There was no recurrence more than 5 years after treatment. All seven local recurrence cases were treated with salvage surgery; however, only one patient was cured. Six of the seven patients with recurrence showed lymph node metastasis during follow-up and three patients died with recurrent tumors. The 2-year nodal control rates were 65% in the 60-Gy arm and 47% in the 54-Gy arm (NS). Nodal metastases occurred in 12 patients in the 60-Gy arm and 9 patients in the 54-Gy arm (Table 2). All but one nodal recurrence occurred within 2 years after brachytherapy. One patient showed lymph node metastasis 61 months after treatment; she showed local recurrence before lymph node metastasis. Of the 22 patients with nodal metastasis, 21 were treated with radical neck dissection (RND) and 1 was treated with radiotherapy for subsequent Rouviere's lymph node metastasis. Eight of the 21 patients treated with RND died with nodal metastasis and/or subsequent distant metastasis, while the other 13 patients were controlled. The patient who was treated with radiotherapy died with nodal metastasis. Ultimately, nodal metastases were controlled in 13 of 22 patients. The 2- and 3-year overall survival rates were both 88% in the 60-Gy arm and 88% and 82% in the 54-Gy arm (n.s.). Four

patients died with nodal metastases in both groups (two with local failure in the 60-Gy arm and one with local recurrence in the 54-Gy arm). One patient died of another cause without any evidence of tongue cancer. As for late complications, tongue ulcers were observed in three patients in each arm. Bone exposure occurred in three patients in the 60-Gy arm and two patients in the 54-Gy arm (Table 2). In detail, 18% and 12% patients in the 54-Gy arm had soft tissue ulcers (4, 8 and 14 months after treatment) and bone exposure, respectively, and 9% and 9% patients in the 60-Gy arm had soft tissue ulcers and bone exposure, respectively. The 1- and 2-year actuarial complication-free rates were 97% and 91%, respectively, in the 60-Gy arm and 83% each in the 54-Gy arm (NS; $P = 0.52$), respectively.

DISCUSSION

Interstitial irradiation is conventionally performed at LDR (2 Gy/h or lower). Many institutes have reported successful results of LDR brachytherapy for tongue cancer [1]. In the 1980s, however, HDR irradiation, performed at a dose rate of 12 Gy/h or higher by remote control, was clinically applied for uterine cancer. Since then, HDR brachytherapy using a remote afterloading technique has been installed in several brachytherapy centers, including ours [3, 4]. HDR hyperfractionated interstitial brachytherapy has the following advantages: (i) accurate calculation enabled by complete fixation of the guide tubes; (ii) parallel source arrangement by the linked double-button technique; (iii) homogeneous dose distribution by stepping source optimization; and (iv) better patient care aided by the elimination of radiation exposure of the medical staff. For those reasons, we have installed HDR brachytherapy through Phase I/II and Phase III studies on head and neck cancer [3, 4].

In some reports, pulsed-dose-rate (PDR) irradiation or daytime PDR was applied for head and neck cancer. Strnad *et al.* reported that PDR interstitial brachytherapy for head and neck cancer gave results comparable with those of LDR brachytherapy [13]. Brenner *et al.* reported the superiority of daytime PDR over continuous LDR [14]. However, if PDR or daytime PDR are used to treat patients with curative intent, a treatment unit must be occupied by the patient for 1 week; moreover, no other patient can be treated with that unit. We have only one HDR remote-controlled afterloading unit with which we treat more than 80 patients per year (mainly uterine, prostate and breast cancer patients). Because of the heavy use of the machine, we cannot use PDR or daytime PDR for patients with head and neck cancer.

Based on a retrospective analysis, Yamazaki *et al.* reported that the 5-year local control rates were compatible between the HDR and LDR groups; the control rates for patients treated solely by brachytherapy were 80% in the LDR group ($n = 341$; T1:T2 = 171:170) and 84% in the HDR group ($n = 58$; T1:T2 = 22:36) [15]. Kakimoto *et al.* reported that the 2- and 3-year local control rates were 67% and 71% for patients with T3 tumors treated with LDR-ISBT and HDR-ISBT, respectively [16]. Therefore the local control rate of patients treated with HDR-ISBT was similar to that of patients treated with LDR-ISBT for T1 to T3 tumors.

In addition, we undertook several efforts to improve HDR-ISBT. To employ a clinical target volume (CTV)-based dose prescription for HDR brachytherapy after CT-based treatment planning installment, Yoshida *et al.* used metal markers in 47 patients (32 with head and neck cancer, 11 with pelvic cancer, 3 with soft tissue cancer and 3 with breast cancer) [17]. At treatment planning, they prescribed and applied a tumoricidal dose to an isodose surface that covered the marked CTV; in addition, they reduced the dose to lower than the constraints for organs at risk. The maximum doses were selected as 80%, 150%, 100%, 50% and 200% of the prescribed doses for the rectum, urethra, mandible, skin and large vessels, respectively. The doses were compared with those calculated by the Paris system theory. If the Paris system (a reference dose of 85% of the basal dose is prescribed to an isodose surface) had been used, 16 patients would have been underdosed and 4 patients (2 with rectal and urethral cancer, 1 with urethral cancer and 1 with large vessel cancer) would have been overdosed. Of the 42 patients treated with doses higher than the tumoricidal dose, 2 had local recurrence, which was also seen in 4 of 7 underdosed patients ($P < 0.0001$). They concluded that metal markers were useful for prescribing tumoricidal doses to CTVs and safety doses to organs at risk. We experienced higher incidence of soft tissue ulcers in the 54-Gy arm (18%) than the 60-Gy arm (9%, NS). We can not explain the reason at present because the same technique had been carried out and no significant differences were found in the long diameter (22 ± 11 mm vs. 23 ± 8 mm), short diameter (17 ± 6 mm vs. 16 ± 4 mm) and thickness (9 ± 10 mm vs. 8 ± 3 mm) between the ulcer positive and negative groups. Dose volume analysis in 3D treatment planning is underway and may shed a light in analyzing this side effect [17]. Following the trends in image innovation, we have tried to fuse magnetic resonance images into computer tomographic images. Further investigation of image guided brachytherapy is warranted.

Some studies have reported that 60 Gy/10 fractions results in a 14% increase compared with 70 Gy LDR in $\alpha/\beta = 10$ and a 54% increase in late responding tissue, which is considered very dangerous [6]. An equivalent dose of HDR-ISBT to 70 Gy of LDR-ISBT was calculated as 48 Gy in late reaction ($\alpha/\beta = 3.8$) and 54 Gy in acute

reaction ($\alpha/\beta = 10$) cases. Therefore we initiated this dose reduction trial to examine whether this strategy is plausible and tactically advantageous if total doses can be reduced without worsening local control rates. As in the present studies no significant differences in outcome were observed between the total doses of 54 Gy and 60 Gy, a total dose of 54 Gy appears to be feasible and was applied thereafter. However, the number of patients in this pilot study was small, and it is difficult to draw firm conclusions. Further studies with a larger number of patients are required.

In conclusion, the outcome of an HDR-ISBT dose of 54 Gy in 9 fractions was similar to that of an HDR-ISBT dose of 60 Gy in 10 fractions in patients with early tongue cancer.

REFERENCES

1. Mazeron JJ, Ardiet JM, Haie-Méder C *et al.* GEC-ESTRO recommendations for brachytherapy for head and neck squamous cell carcinomas. *Radiother Oncol* 2009;**91**:150–6.
2. Shigematsu Y, Masaki N, Ikeda H *et al.* Current status and future of brachytherapy. *Gan No Rinsho* 1983;**29**:695–701 (in Japanese).
3. Teshima T, Inoue T, Ikeda H *et al.* Phase I/II study of high-dose rate interstitial radiotherapy for head and neck cancer. *Strahlenther Onkol* 1992;**168**: 617–21.
4. Inoue Ta, Inoue To, Yoshida K *et al.* Phase III trial of high vs. low dose rate interstitial radiotherapy for mobile tongue cancer. *Int J Radiat Oncol Biol Phys* 2001;**51**:171–75.
5. Lau HY, Hay J, Flores A *et al.* Seven fractions of twice daily high dose-rate brachytherapy for node-negative carcinoma of the mobile tongue results in loss of therapeutic ratio. *Radiother Oncol* 1996;**391**:15–18.
6. Leung TW, Wong VY, Kwan KH *et al.* High dose rate brachytherapy for early stage oral tongue cancer. *Head Neck* 2002;**243**:274–81.
7. Rudoltz MS, Perkins RS, Luthmann RW *et al.* High-dose-rate brachytherapy for primary carcinomas of the oral cavity and oropharynx. *Laryngoscope* 1999;**109**:1967–73.
8. Patra NB, Goswami J, Basu S *et al.* Outcomes of high dose rate interstitial boost brachytherapy after external beam radiation therapy in head and neck cancer—an Indian (single institutional) learning experience. *Brachytherapy* 2009;**8**: 248–54.
9. Guinot JL, Santos M, Tortajada MI *et al.* Efficacy of high-dose-rate interstitial brachytherapy in patients with oral tongue carcinoma. *Brachytherapy* 2010;**9**:227–34.
10. Petera J, Matula P, Paluska P *et al.* High dose rate versus LDR brachytherapy in the treatment of tongue carcinoma—a radiobiological study. *Neoplasma* 2009;**56**:163–8.
11. Nag S, Cano ER, Demanes D *et al.* The American Brachytherapy Society recommendations for high-dose-rate brachytherapy for head-and-neck carcinoma. *Int J Radiat Oncol Biol Phys* 2001;**50**:1190–98.
12. Mochizuki S, Kanehira C, Sekine H *et al.* A study on optimum time-dose relationship in high dose rate interstitial radiotherapy. *Jpn J Clin Radiol* 1994;**39**:1151–54.
13. Strnad V, Lotter M, Grabenbauer G *et al.* Early results of pulsed-dose-rate interstitial brachytherapy for head and neck malignancies after limited surgery. *Int J Radiat Oncol Biol Phys* 2000;**46**:27–30.
14. Brenner DJ, Schiff PB, Huang Y *et al.* Pulsed-dose-rate brachytherapy: Design of convenient (daytime-only) schedule. *Int J Radiat Oncol Biol Phys* 1997;**39**:809–15.
15. Yamazaki H, Inoue T, Yoshida K *et al.* Brachytherapy for early oral tongue cancer: LDR to high dose rate. *J Radiat Res* 2003;**44**:37–40.
16. Kakimoto N, Inoue T, Inoue T *et al.* Results of low- and high-dose-rate interstitial brachytherapy for T3 mobile tongue cancer. *Radiother Oncol* 2003;**68**:123–8.
17. Yoshida K, Nose T, Koizumi M *et al.* The usefulness of metal markers for CTV-based dose prescription in high-dose-rate interstitial brachytherapy. *J Jpn Soc Ther Radiol Oncol* 2002;**13**:253–60.

International Journal of
Radiation Oncology
biology • physics

www.redjournal.org

Clinical Investigation

Dose-Volume Histogram Predictors of Chronic Gastrointestinal Complications After Radical Hysterectomy and Postoperative Concurrent Nedaplatin-Based Chemoradiation Therapy for Early-Stage Cervical Cancer

Fumiaki Isohashi, MD, PhD,* Yasuo Yoshioka, MD, PhD,* Seiji Mabuchi, MD, PhD,† Koji Konishi, MD, PhD,* Masahiko Koizumi, MD, PhD,*,‡ Yutaka Takahashi, PhD,*,‡ Toshiyuki Ogata, PhD,*,‡ Shintaroh Maruoka, MD,* Tadashi Kimura, MD, PhD,† and Kazuhiko Ogawa, MD, PhD*

*Departments of *Radiation Oncology and †Obstetrics and Gynecology, ‡Division of Medical Physics, Oncology Center, Osaka University Hospital, Suita, Osaka, Japan*

Received Jan 24, 2012, and in revised form May 1, 2012. Accepted for publication May 10, 2012

Summary

In this study, dose-volume histogram parameters of the small bowel loops were predictive for the development of chronic gastrointestinal (GI) complications after postoperative concurrent nedaplatin-based chemoradiation therapy for early-stage cervical cancer. Multivariate analysis indicated that V40 (volume receiving more than 40 Gy) of the small bowel loops and smoking were independent predictors of GI complications.

Purpose: The purpose of this study was to evaluate dose-volume histogram (DVH) predictors for the development of chronic gastrointestinal (GI) complications in cervical cancer patients who underwent radical hysterectomy and postoperative concurrent nedaplatin-based chemoradiation therapy.

Methods and Materials: This study analyzed 97 patients who underwent postoperative concurrent chemoradiation therapy. The organs at risk that were contoured were the small bowel loops, large bowel loop, and peritoneal cavity. DVH parameters subjected to analysis included the volumes of these organs receiving more than 15, 30, 40, and 45 Gy (V15-V45) and their mean dose. Associations between DVH parameters or clinical factors and the incidence of grade 2 or higher chronic GI complications were evaluated.

Results: Of the clinical factors, smoking and low body mass index (BMI) (<22) were significantly associated with grade 2 or higher chronic GI complications. Also, patients with chronic GI complications had significantly greater V15-V45 volumes and higher mean dose of the small bowel loops compared with those without GI complications. In contrast, no parameters for the large bowel loop or peritoneal cavity were significantly associated with GI complications. Results of the receiver operating characteristics (ROC) curve analysis led to the conclusion that V15-V45 of the small bowel loops has high accuracy for prediction of GI complications. Among these parameters, V40 gave the highest area under the ROC curve. Finally, multivariate analysis was performed with V40 of the small bowel loops and 2 other clinical parameters that were judged to be potential risk factors for chronic GI complications: BMI and smoking. Of these 3 parameters, V40 of the small bowel loops and smoking emerged as independent predictors of chronic GI complications.

Reprint requests to: Fumiaki Isohashi, Department of Radiation Oncology, Osaka University Graduate School of Medicine, 2-2 (D10) Yamadaoka, Suita, Osaka 565-0871, Japan. Tel: (+81) 6-6879-3482; Fax: (+81) 6-6879-3489; E-mail: isohashi@radonc.med.osaka-u.ac.jp

Conflict of interest: none.

Int J Radiation Oncol Biol Phys, Vol. ■, No. ■, pp. 1–7, 2012
0360-3016/$ - see front matter
doi:10.1016/j.ijrobp.2012.05.021

Conclusions: DVH parameters of the small bowel loops may serve as predictors of grade 2 or higher chronic GI complications after postoperative concurrent nedaplatin-based chemoradiation therapy for early-stage cervical cancer. © 2012 Elsevier Inc.

Introduction

Adjuvant whole-pelvic radiation therapy (RT) after radical hysterectomy reduces locoregional recurrence in cervical cancer patients after surgery with adverse risk factors (1, 2). However, patients undergoing whole-pelvic RT after radical hysterectomy may suffer severe gastrointestinal (GI) complications with an incidence varying from 3%-13% for patients treated with pelvic RT alone (1-3). Moreover, while adjuvant concurrent chemoradiation therapy has been shown in several studies to improve survival rates for high-risk cervical cancer patients compared with adjuvant RT alone, GI complications were observed more frequently in conjunction with concurrent chemoradiation therapy than with RT alone (4). Therefore it is important to improve the feasibility of adjuvant concurrent chemoradiation therapy by reducing GI complications.

Because the small bowel is one of the critical organs involved in GI complications, a predictive model of acute GI complications of the small bowel has been established with the aid of Quantitative Analyses of Normal Tissue Effects in the Clinic (QUANTEC) (5). However, the correlation between dose-volume effect and chronic GI complications of the small bowel has not been extensively investigated.

Since 2000, we have been using postoperative concurrent nedaplatin-based chemoradiation therapy for early-stage cervical cancer patients with adverse risk factors (6). The purpose of the study reported here was to evaluate dose-volume histogram (DVH) predictors for the development of chronic GI complications in cervical cancer patients who underwent radical hysterectomy and postoperative concurrent nedaplatin-based chemoradiation therapy.

Methods and Materials

Patients

A total of 131 patients with cervical cancer received radical hysterectomy and postoperative RT at our institute between April 2000, when we started to use postoperative concurrent nedaplatin-based chemoradiation therapy, and September 2010. Treatment criteria for postoperative RT were previously described (6, 7). Thirty-four of these patients were excluded from the study: 18 who received extended-field radiation therapy alone because of multiple lymph node metastases (7), 9 who refused concurrent chemotherapy, 3 who received intracavitary brachytherapy with whole-pelvic RT because of a close surgical margin, and 4 early patients who did not undergo radiation treatment planning computed tomography (CT) with a 2-dimensional (2D) era. The remaining 97 patients treated with concurrent chemoradiation therapy were analyzed for this study with a minimum follow-up period of 3 months. This study was approved by our institutional review board.

Radiation therapy and chemotherapy

Whole-pelvic RT was delivered with 2D planning in 65 patients between April 2000 and March 2008 and with 3-dimensional (3D) conformal treatment planning in 32 patients starting April 2008. During the 2D era, RT was delivered using 10-megavolt X rays from a linear accelerator with the anteroposterior parallel opposing technique. The superior margin of the whole-pelvic RT was at the upper edge of the fifth lumbar vertebra and the inferior margin was the inferior edge of the obturator foramen. Laterally, the field extended 2 cm beyond the lateral margins of the bony pelvic wall. After we defined an isocenter or field-shape in the X-ray simulator, CT with the isocenter position marked was performed with 5.0-mm slices without filling the bladder to calculate the monitor unit and check the dose distribution. The CT scan range was from the upper edge of L3 to at least 7 cm below the bottom of the obturator foramen. The dose distribution was calculated using a commercial treatment planning system (FOCUS; Elekta, Stockholm Sweden). The prescribed RT doses were 50 Gy administered in 25 fractions over 5 weeks at the center of the body. Multileaf collimators were used to block the upper and lower corners of the radiation field. No target volume or organ at risk was delineated before treatment. Since April 2008, all patients have been treated with 3D conformal treatment planning. RT planning CT was performed with 2.5-mm slices with normal quiet breathing and a full-bladder scan. The CT scan range was the same as that used in 2D planning. A commercial treatment planning system (XiO TPS; Elekta) was used to design the radiation fields. The clinical target volume (CTV) comprised a central vaginal CTV and a regional nodal CTV. The former included the proximal vagina and paravaginal tissues and the latter consisted of the common iliac, external and internal iliac, and presacral lymph nodes. CTVs were contoured according to the consensus guidelines of the Radiation Therapy Oncology Group (RTOG) 0418 (8) and its atlas on the RTOG website. The planning target volume (PTV) was generated by using 1.0-cm uniform expansion of the CTV. The prescribed RT doses were 50 Gy at the center of the PTV, administered in 25 fractions over 5 weeks by means of the 3D 4-field box technique. Multileaf collimators were used to cover the PTV with a margin of approximately 5 mm. No organ at risk was delineated before treatment. Nedaplatin (40 mg/m^2) was given intravenously on a weekly basis during the course of whole-pelvic RT for 5 weeks as previously described (6).

Contouring and evaluation of normal structures

The organs at risk that were contoured comprised the small bowel loops, large bowel loop, and peritoneal cavity. All contouring was done retrospectively. The superior and inferior extents of critical organs were outlined on all CT slices containing portions of the PTV (3D) or field margins (2D), including an additional area 2-cm superior and inferior to the limit of the PTV or field margins. Therefore, the organs at risk, including the large bowel loop, small bowel loops, and peritoneal cavity, could not be contoured in full volume. The large bowel loop was contoured first as a single loop continuing from the end of the sigmoid colon to the ascending colon, and the remaining bowel loops were classified as the small bowel loops. A preoperative diagnostic CT scan using oral and intravenous contrast media was performed in 92/97 patients (95%). This preoperative CT scan

was displayed when the organs at risk were contoured using postoperative radiation treatment planning CT. Diagnostic CT images were not fused to the planning scans. In the remaining 5 patients, postoperative radiation treatment planning CT only was used for contouring of the organs at risk. The peritoneal cavity was defined as including the volume surrounding the small bowel loops out to the edge of the peritoneum. The boundaries included the abdominal wall anteriorly and anterolaterally, the retroperitoneal and deep pelvic muscles posterolaterally, and the great vessels, vertebral bodies, and sacrum posteriorly. The rectum and bladder were excluded from the peritoneal cavity volume. DVH parameters subjected to analysis included the mean doses to the small bowel loops, large bowel loop, and peritoneal cavity, and the volumes of these organs receiving more than 15, 30, 40, and 45 Gy (V15-V45).

Follow-up and evaluation of chronic GI complications

The patients were followed up by gynecologic and radiation oncologists on an outpatient basis every month in the first year, every 2 months in the second year, every 3 months in the third year, every 4 months in the fourth year, every 6 months in the fifth year, and annually thereafter until 10 years after treatment. We defined a chronic complication as a GI event that occurred more than 3 months after radiation therapy was started. The severity of the GI complication was classified according to the RTOG/European Organization for Research and Treatment of Cancer Late Radiation Morbidity Score. Toxicity data including the grade of GI complications were collected retrospectively through hospitalization and follow-up records.

Statistical analysis

Associations between selected DVH parameters (V15, V30, V40, V45, and mean dose) and the incidence of grade 2 or higher chronic GI complications were evaluated. The relationships between clinical or DVH parameters and the incidence of chronic GI complications were analyzed with the Mann-Whitney *U* test for quantitative variables and the Fisher exact test for categorical variables. The mean DVH parameters for the small bowel loops, large bowel loop, and peritoneal cavity of patients with and without GI complications were compared by Mann-Whitney *U* test. Receiver operating characteristics (ROC) curve analysis of each of the DVH parameters was performed to select the most relevant threshold for prediction of a grade 2 or higher chronic GI complication. The predictive value of a parameter was evaluated based on the area under the ROC curve (AUC). The AUC reflects the ability of the test to distinguish between patients with and without disease. The optimal threshold for each DVH parameter was defined as the point yielding the minimal value for $(1 - \text{sensitivity})^2 + (1 - \text{specificity})^2$, which is the point on the ROC curve closest to the upper left-hand corner (9). Multivariate analysis using Cox regression models was performed to identify risk factors associated with grade 2 or higher chronic GI complications. The actuarial incidence of GI complications was calculated with the Kaplan-Meier method and differences between groups were compared by log-rank test. A P value of $<.05$ or a 95% confidence interval not encompassing 1 was considered to be statistically significant. All statistical tests were 2-sided.

Results

The characteristics of the 97 patients are shown in Table 1. The median follow-up period from the start of radiation therapy was 43 months (range 4-111 months). None of the patients experienced a local or distant recurrence within 3 months. The Eastern Cooperative Oncology Group performance status was 0-1 for all patients. The median age of the patients was 51 years old (range 28-70 years old). Twenty-three patients (24%) had a history of smoking, with a median Brinkman index (number of cigarettes per day × smoking years) of 400 (range 100-1200). The median total dose of nedaplatin was 285 mg (range 30-375 mg). Ninety-two patients (95%) received the whole RT dose as planned (50 Gy), but 3 patients (3%) received only 46 Gy and 2 (2%) received 44 Gy because of neutropenia (4 patients) or patient refusal (1 patient). Eighty-one patients (84%) had grade 0-1, 6 (6%) had grade 2, and 10 (10%) had grade 3 chronic GI

Table 1 Patient and treatment characteristics

	No. (%)
Age (y)	
Mean	51
SD	±10
T-stage	
T1	53 (55)
T2	44 (45)
N-stage	
N0	64 (66)
N1	33 (34)
Histology	
SCC	71 (73)
Ad	24 (25)
Others	2 (2)
Smoking	
None	74 (76)
Yes	23 (24)
Diabetes	
None	94 (97)
Yes	3 (3)
Abdominopelvic surgery	
None	94 (97)
Yes	3 (3)
BMI (kg/m^2)	
Mean	21.6
SD	±3.8
RT total dose (Gy)	
50	92 (95)
46	3 (3)
44	2 (2)
RT technique	
2D	65 (67)
3D	32 (33)
Total nedaplatin (mg)	
Mean	274
SD	±52

Abbreviations: 2D = 2-dimensional; 3D = 3-dimensional; Ad = adenocarcinoma; BMI = body mass index; RT = radiation therapy; SCC = squamous cell carcinoma; SD = standard deviation.

Table 2 Univariate analysis (Mann-Whitney *U* test and Fisher exact test) for the development of grade 2 or higher chronic GI complications

	Grade 0-1	Grade 2-3	
Variable	No.	No.	*P* value
Age (y)			
<52	39	10	.294
≥52	42	6	
Total nedaplatin (mg)			
<285	39	8	.892
≥285	42	8	
T-stage			
T1	46	7	.338
T2	35	9	
N-stage			
N0	53	11	.798
N1	28	5	
Histology			
SCC	60	11	.660
Non-SCC	21	5	
RT total dose			
50 Gy	76	16	.308
<50 Gy	5	0	
RT technique			
2D	57	8	.133
3D	24	8	
Smoking			
None	66	8	.005
Yes	15	8	
BMI (kg/m^2)			
<22	43	14	.011
≥22	38	2	

Abbreviations: 2D = 2-dimensional; 3D = 3-dimensional; BMI = body mass index; GI = gastrointestinal; RT = radiation therapy; SCC = squamous cell carcinoma.

Table 3 Comparison of mean DVH parameters of the small bowel loops, large bowel loop, and peritoneal cavity in patients with and without chronic GI complications (Mann-Whitney *U* test)

	Overall	Grade 0-1	Grade 2-3	*P* value
		Small bowel loops		
		Mean volume ± SE (mL)		
V15	337 ± 15	299 ± 13	527 ± 37	<.001
V30	308 ± 13	273 ± 11	485 ± 29	<.001
V40	289 ± 13	255 ± 11	458 ± 27	<.001
V45	280 ± 12	247 ± 11	444 ± 26	<.001
		Mean dose (cGy ± SE)		
	3,523 ± 80	3,429 ± 86	3,994 ± 160	<.001
		Large bowel loop		
		Mean volume ± SE (mL)		
V15	241 ± 12	241 ± 12	239 ± 34	.730
V30	207 ± 10	210 ± 11	192 ± 23	.550
V40	183 ± 10	189 ± 11	156 ± 17	.331
V45	176 ± 9	182 ± 10	149 ± 16	.321
		Mean dose (cGy ± SE)		
	2,747 ± 62	2,768 ± 66	2,639 ± 174	.487
		Peritoneal cavity		
		Mean volume ± SE (mL)		
V15	1,151 ± 29	1,129 ± 32	1,262 ± 70	.111
V30	1,045 ± 25	1,027 ± 27	1,138 ± 64	.174
V40	974 ± 25	960 ± 27	1,049 ± 65	.336
V45	941 ± 24	927 ± 26	1,013 ± 65	.343
		Mean dose (cGy ± SE)		
	3,421 ± 47	3,387 ± 50	3,596 ± 122	.169

Abbreviations: DVH = dose-volume histogram; GI = gastrointestinal; SE = standard error; V15-45 = volume receiving more than respective dose.

complications. Of the 10 patients with grade 3 GI complications, 5 (5% of all patients) had small bowel obstruction requiring surgery.

The incidence of chronic GI complications was analyzed as a function of clinical factors. Because there were few patients with diabetes or a history of abdominopelvic surgery among the study population, we did not analyze these factors. The results of univariate analyses are shown in Table 2. Smoking habit and low body mass index (BMI; <22) were significantly associated with grade 2 or higher GI complications. The mean DVH parameters of the small bowel loops, large bowel loop, and peritoneal cavity of patients with and without GI complications are shown in Table 3. Patients with grade 2 or higher GI complications had significantly greater V15-V45 volumes in the small bowel loops than did those without GI complications ($P<.001$). The mean dose to the small bowel loops differed significantly for patients with and without GI complications (39.94 vs 34.29 Gy, $P<.001$). In contrast, none of the parameters for the large bowel loop or peritoneal cavity were significantly associated with GI complications.

ROC curve analysis was performed to select the most relevant parameter to identify predictors of grade 2 or higher chronic GI complications among DVH parameters for the small bowel loops. The results are shown in Table 4. Because AUCs for mean dose, V15, V30, V40, and V45 were 0.693, 0.909, 0.912, 0.921, and 0.890, respectively, indicating that V15-V45 have good accuracy for prediction of GI complications. Strong collinearity among V15-V45 was expected in multivariate

Table 4 ROC curve analysis for DVH parameters of small bowel loops in relation to grade 2 or higher chronic GI complications

			Optimal threshold	
	AUC	95% CI	Value	Sensitivity/specificity (%)
Mean dose	0.693	0.580-0.806	3600 cGy	62.5/62.5
V15	0.909	0.855-0.963	380 mL	93.8/82.1
V30	0.912	0.857-0.967	360 mL	93.8/82.1
V40	0.921	0.869-0.972	340 mL	87.5/87.2
V45	0.890	0.819-0.962	340 mL	87.5/85.1

Abbreviations: AUC = area under the ROC curve; CI = confidence interval; DVH = dose-volume histogram; GI = gastrointestinal; ROC = receiver operating characteristics; V15-45 = volume receiving more than respective dose.

Table 5 Multivariate analysis for the development of grade 2 or higher chronic GI complications

Variable	HR (95% CI)	*P* value
V40 of small bowel loops (mL)	1.012 (1.007-1.018)	<.001
BMI (<22 vs ≥22)	3.024 (0.585-15.622)	.187
Smoking (yes vs no)	3.103 (1.023-9.415)	.046

Abbreviations: BMI = body mass index; CI = confidence interval; GI = gastrointestinal; HR = hazard ratio; V40 = volume receiving more than 40 Gy.

analysis. Therefore, we used V40 of the small bowel loops in multivariate analysis because this parameter had the highest AUC value. The optimal threshold for V40 was 340 mL. Thus, multivariate analysis was performed with V40 of the small bowel loops and 2 other clinical parameters that were judged to be potential risk factors for chronic GI complications: BMI and smoking habit. Of these 3 parameters, V40 of the small bowel loops and smoking emerged as independent predictors of GI complications (Table 5).

The overall incidences of grade 2 or higher GI complications were 0% (0/39), 7% (2/29), and 48% (14/29) for patients with V40 values of <250 mL, 250-340 mL, and >340 mL, respectively. Thus, the overall incidence of grade 2 or higher GI complications increased in a volume-dependent manner. Therefore, we performed Kaplan-Meier estimates of the cumulative incidence curves for grade 2 or higher chronic GI complications stratified by V40 of the small bowel loops using the above intervals. The cumulative incidence curves for grade 2 or higher chronic GI complications stratified by V40 of the small bowel loops are shown in Fig. The 3-year cumulative incidences of grade 2 or higher GI complications were 0%, 8.4%, and 46.2% for patients with V40 values of <250 mL, 250-340 mL, and >340 mL, respectively, with a significantly higher risk for patients with V40 > 340 mL than for the other groups ($P<.001$).

Discussion

Several previous studies have introduced predictive factors potentially associated with chronic GI complications after RT for gynecologic malignancies employing several types of therapy (3, 10-14). These factors include total RT dose, RT dose per fraction, history of diabetes, acute toxicity, BMI, age, previous abdominopelvic surgery, and smoking. In our study, smoking and low BMI were identified by univariate analysis as predictors of GI complications. Moreover, the V15-V45 volumes and the mean dose of the small bowel loops all showed a significant association with chronic GI complications. In addition, multivariate analysis identified V40 of the small bowel loops and smoking as independent predictors of GI complications. To the best of our knowledge, ours is the first study to show that DVH parameters of the small bowel loops derived with an up-to-date approach are associated with chronic GI complications after postoperative concurrent chemoradiation therapy for cervical cancer.

We believe that our findings are important for the practice of the radiation oncology, because adverse events caused by radiation exposure, such as GI complications, may be relieved by using an appropriate radiation technique or a mechanical device such as a belly-board. Recently, intensity modulated radiation therapy (IMRT) has emerged as a sophisticated technique for treatment of tumor regions or areas at risk of recurrence, while sparing adjacent normal tissue from high-dose irradiation, including in patients with gynecological cancer treated with IMRT after radical hysterectomy (15-18).

Two methods for contouring the small bowel volume have been reported: one uses direct delineation of the individual loops, whereas the other bases delineation on the peritoneal cavity because the bowel may lie within this space at any time throughout the course of treatment (5). Because these methods have not been compared to determine which leads to better predictions of chronic complications of the small bowel, we established separate parameters for the irradiated volume of the small bowel loops and the peritoneal cavity to examine which parameters correlated with

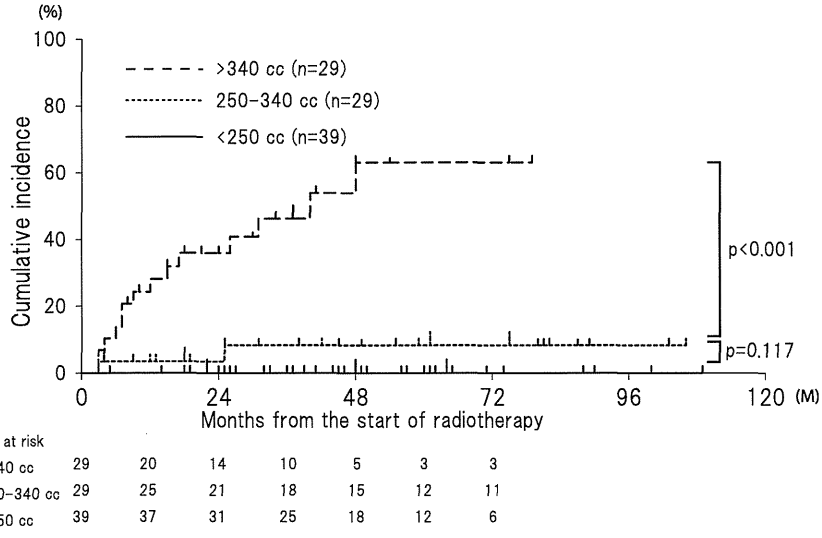

Fig. Kaplan-Meier estimates of cumulative incidence curves for grade 2 or higher chronic gastrointestinal (GI) complications stratified by V40 of the small bowel loops. The 3-year cumulative incidences of grade 2 or higher GI complications were 0%, 8.4%, and 46.2% for patients with V40 values of <250 mL, 250-340 mL, and >340 mL, respectively, with a significantly higher risk for patients with V40 > 340 mL than for the other groups (log-rank test; $P<.001$).

development of chronic GI complications. Interestingly, patients with grade 2 or higher chronic GI complications featured significantly higher V15-V45 volumes and mean dose to the small bowel loops than did patients without this feature. In contrast, none of the parameters for the peritoneal cavity showed any association with chronic GI complications. Similarly, parameters for the large bowel did not correlate with radiation-induced chronic GI complications. These findings suggest that, compared to the peritoneal cavity, the small bowel loops may constitute a better predictor of chronic GI complications. However, it is also likely that the dose to the peritoneal cavity will be a predictor of acute GI complications (5), and Wedlake et al found that cumulative acute GI symptoms, measured using the questionnaire, are associated with consequential late symptoms (14). Collectively, these results suggest that our finding that parameters for the small bowel loops are better predictors of chronic GI complication, compared with those for the peritoneal cavity, requires verification in larger prospective studies.

The findings in this study should be interpreted with an understanding of the following limitations. First, the heterogeneity in the treatment planning approach over the period of the study (2D vs 3D), the low number of events, and the lack of a prespecified model or protocol are important limitations of the data and analysis. Second, our method resulted in large uniform doses to regions of the small bowel, which differ from the dose patterns produced by techniques such as IMRT, which is becoming more prevalent. Therefore, we cannot exclude the possibility that the optimal DVH parameter predictors found in this study may differ from those for IMRT.

Additionally, we used weekly nedaplatin as concurrent chemotherapy, whereas chemoradiation therapy with 40 mg/m^2 of weekly cisplatin is now accepted as a standard first-line treatment. We therefore cannot exclude the possibility that the optimal DVH parameter predictors found in the study may be chemotherapy-type specific. Furthermore, the small bowel DVH parameters were estimated based on only 1 radiation treatment planning CT before RT, while in fact daily variability of the distention or movement of the small bowels during the treatment course may have affected the dose-volume profile. Also, especially in the 2D era, radiation treatment planning CT performed with 5.0-mm slices without filling the bladder may not reflect the actual dose received. Han et al reported that the dose distribution in the small bowel as observed on CT varies significantly from week to week because of the interfractional variations of small-bowel positions (19). In addition, image guided RT is now widely used in many institutions (20). Therefore, further studies using image guided RT will be necessary to investigate the influence of intra- and interfraction motion of the small bowel loops on chronic GI complications.

Within these limitations, we conclude that DVH parameters of the small bowel loops may serve as predictors of chronic GI complications of grade 2 or higher after postoperative concurrent nedaplatin-based chemoradiation therapy in early-stage cervical cancer patients. For these patients, we recommend that V40 of the small bowel loops should be <340 mL to avoid chronic GI complications using a conventional 2D or 3D technique.

References

1. Sedlis A, Bundy BN, Rotman MZ, Lentz SS, Muderspach LI, Zaino RJ. A randomized trial of pelvic radiation therapy versus no further therapy in selected patients with stage IB carcinoma of the cervix after radical hysterectomy and pelvic lymphadenectomy: a Gynecologic Oncology Group Study. *Gynecol Oncol* 1999;73:177-183.
2. Fiorica JV, Roberts WS, Greenberg H, Hoffman MS, LaPolla JP, Cavanagh D, et al. Morbidity and survival patterns in patients after radical hysterectomy and postoperative adjuvant pelvic radiotherapy. *Gynecol Oncol* 1990;36:343-347.
3. Chen SW, Liang JA, Yang SN, Hung YC, Yeh LS, Shiau AC, et al. Radiation injury to intestine following hysterectomy and adjuvant radiotherapy for cervical cancer. *Gynecol Oncol* 2004;95:208-214.
4. Peters WA 3rd, Liu PY, Barrett RJ 2nd, Stock RJ, Monk BJ, Berek JS, et al. Concurrent chemotherapy and pelvic radiation therapy compared with pelvic radiation therapy alone as adjuvant therapy after radical surgery in high-risk early-stage cancer of the cervix. *J Clin Oncol* 2000;18:1606-1613.
5. Kavanagh BD, Pan CC, Dawson LA, Das SK, Li XA, Ten Haken RK, et al. Radiation dose-volume effects in the stomach and small bowel. *Int J Radiat Oncol Biol Phys* 2010;76(Suppl. 3):S101-S107.
6. Mabuchi S, Morishige K, Isohashi F, Yoshioka Y, Takeda T, Yamamoto T, et al. Postoperative concurrent nedaplatin-based chemoradiotherapy improves survival in early-stage cervical cancer patients with adverse risk factors. *Gynecol Oncol* 2009;115:482-487.
7. Mabuchi S, Okazawa M, Isohashi F, Ohta Y, Maruoka S, Yoshioka Y, et al. Postoperative whole pelvic radiotherapy plus concurrent chemotherapy versus extended-field irradiation for early-stage cervical cancer patients with multiple pelvic lymph node metastases. *Gynecol Oncol* 2011;120:94-100.
8. Small W Jr., Mell LK, Anderson P, Creutzberg C, De Los Santos J, Gaffney D, et al. Consensus guidelines for delineation of clinical target volume for intensity-modulated pelvic radiotherapy in postoperative treatment of endometrial and cervical cancer. *Int J Radiat Oncol Biol Phys* 2008;71:428-434.
9. Akobeng AK. Understanding diagnostic tests 3: receiver operating characteristic curves. *Acta Paediatr* 2007;96:644-647.
10. Iraha S, Ogawa K, Moromizato H, Shiraishi M, Nagai Y, Samura H, et al. Radiation enterocolitis requiring surgery in patients with gynecological malignancies. *Int J Radiat Oncol Biol Phys* 2007;68:1088-1093.
11. Kasuya G, Ogawa K, Iraha S, Nagai Y, Shiraishi M, Hirakawa M, et al. Severe late complications in patients with uterine cancer treated with postoperative radiotherapy. *Anticancer Res* 2011;31:3527-3533.
12. Eifel PJ, Jhingran A, Bodurka DC, Levenback C, Thames H. Correlation of smoking history and other patient characteristics with major complications of pelvic radiation therapy for cervical cancer. *J Clin Oncol* 2002;20:3651-3657.
13. Kizer NT, Thaker PH, Gao F, Zighelboim I, Powell MA, Rader JS, et al. The effects of body mass index on complications and survival outcomes in patients with cervical carcinoma undergoing curative chemoradiation therapy. *Cancer* 2011;117:948-956.
14. Wedlake LJ, Thomas K, Lalji A, Blake P, Khoo VS, Tait D, et al. Predicting late effects of pelvic radiotherapy: is there a better approach? *Int J Radiat Oncol Biol Phys* 2010;78:1163-1170.
15. Roeske JC, Lujan A, Rotmensch J, Waggoner SE, Yamada D, Mundt AJ. Intensity-modulated whole pelvic radiation therapy in patients with gynecologic malignancies. *Int J Radiat Oncol Biol Phys* 2000;48:1613-1621.
16. Jhingran A, Winter K, Portelance L, Miller BE, Salehpour M, Gaur R, et al. A phase II study of intensity modulated radiation therapy (IMRT) to the pelvic for post-operative patients with endometrial carcinoma (RTOG 0418). *Int J Radiat Oncol Biol Phys* 2008;72:S16.
17. Mundt AJ, Mell LK, Roeske JC. Preliminary analysis of chronic gastrointestinal toxicity in gynecology patients treated with intensity-modulated whole pelvic radiation therapy. *Int J Radiat Oncol Biol Phys* 2003;56:1354-1360.
18. Chen MF, Tseng CJ, Tseng CC, Kuo YC, Yu CY, Chen WC. Clinical outcome in posthysterectomy cervical cancer patients treated with

concurrent Cisplatin and intensity-modulated pelvic radiotherapy: comparison with conventional radiotherapy. *Int J Radiat Oncol Biol Phys* 2007;67:1438-1444.

19. Han Y, Shin EH, Huh SJ, Lee JE, Park W. Interfractional dose variation during intensity-modulated radiation therapy for cervical cancer assessed by weekly CT evaluation. *Int J Radiat Oncol Biol Phys* 2006; 65:617-623.
20. Simpson DR, Lawson JD, Nath SK, Rose BS, Mundt AJ, Mell LK. A survey of image-guided radiation therapy use in the United States. *Cancer* 2010;116:3953-3960.